

Electron transport through correlated molecules computed using the time-independent Wigner function: Two critical tests

Ioan Bâldea* and Horst Köppel

Theoretische Chemie, Physikalisch-Chemisches Institut, Universität Heidelberg, Im Neuenheimer Feld 229, D-69120 Heidelberg, Germany

(Received 4 June 2008; published 19 September 2008)

We have implemented the linear response approximation of a method proposed to compute the electron transport through correlated molecules based on the time-independent Wigner function [P. Delaney and J. C. Greer, *Phys. Rev. Lett.* **93**, 036805 (2004)]. The results thus obtained for the zero-bias conductance through a quantum dot both without and with correlations demonstrate that this method is neither quantitatively nor qualitatively able to provide a correct physical description of the electric transport through nanosystems. We present an analysis indicating that the failure is due to the manner of imposing the boundary conditions and that it cannot be simply remedied.

DOI: [10.1103/PhysRevB.78.115315](https://doi.org/10.1103/PhysRevB.78.115315)

PACS number(s): 73.63.Kv, 73.23.Hk

I. INTRODUCTION

Electronic transport in artificial nanosystems and single molecules represents a topic of continuing current interest and remains a challenge both for fundamental science and technological applications. In spite of numerous advances, there still exist important issues which are far from being resolved. Notoriously, the comparison between experimental and theoretical values for the current flowing through molecules usually shows large discrepancies, typically several orders of magnitude.^{1–3} No consensus has been reached so far whether the discrepancies are to be attributed to uncontrollable experimental factors (compare measurements on same systems in Refs. 4–7) or inadequate theoretical frameworks.

Early theoretical calculations were carried out within the Landauer formalism,^{8,9} which is based on a single-particle description. Because systematically the values of the currents thus obtained are at odds with those experimentally measured, a series of theoretical methods was developed to treat electron correlations, which are excluded by the Landauer approach.

The description of electron correlation represents an important challenge from the theoretical side. The most popular theoretical approaches for nonequilibrium transport in correlated nanoscopic/molecular systems are based on nonequilibrium Green functions (NEGF),^{10,11} time-dependent density matrix renormalization group (DMRG),^{12–14} and numerical renormalization group (NRG).¹⁵ In *ab initio* modeling of molecular electronics, the NEGF technique is by far the most utilized one. It is usually combined with electron structure calculations based on density functional theories (DFTs).^{16–18} The NEGF+DFT approach is conceptually simple and computationally less demanding than many-body methods.^{19–24} However, because of the incompletely elucidated current dependence^{25,26} and self-interaction corrections^{27,28} of the local exchange and correlation functionals, the DFT currents can sensitively vary by choosing different approximate potentials.

Out of the methods proposed so far, the method proposed in Ref. 21 seems to be one of the most appealing because of

its claim to correctly reproduce the steady-state current experimentally measured through correlated molecular systems. It relies upon genuine many-body calculations and is not limited to a particular configuration interaction (CI), e.g., restricted to singly, doubly, or triply excited configurations. The originality of this approach consists in the manner of imposing the boundary conditions. Rather than the Fermi distribution function, the Wigner distribution function is employed instead for the constrains at the device-electrode (reservoirs) interfaces. Unlike the former, which is meaningful only within a single-particle picture, the latter can be directly used in a many-body approach. Because the key quantity of this method is the stationary Wigner function (SWF), hereafter it will be referred to as the SWF method.

One should emphasize from the very beginning that the support of the SWF method, and especially its manner to impose boundary conditions, entirely relies upon its ability to provide currents comparable with those measured experimentally for two molecular systems^{21,29} and plausible results for another class of molecules.³⁰ Because this method is conceptually so different from the other widely utilized approaches, it would be highly desirable to inquire the validity of this method within the realm of theory. If and to the extent to which the SWF method is able to reproduce well established results, one can consider its predictions reliable. It is the purpose of the present work to investigate whether the SWF method is able to correctly describe nanosystems whose behavior is well understood.

The remaining part of the paper is organized in the following manner. The theoretical framework, the linear response approximation of the SWF method, will be developed in Sec. II. The model for the “device” we shall consider, consisting of a single quantum dot (QD), will be exposed in Sec. III. Next, in Sec. IV, we shall compare the zero-bias conductance calculated without correlations by means of the SWF method with the exact one. Section V will be devoted to the linear transport through the QD in the presence of correlations. The implications of our results will be discussed in Sec. VI. Conclusions will be presented in Sec. VII.

II. METHOD

Theoretical studies of the transport in nanosystems are inherently faced with the problem of separating the total system (\mathcal{S}) into left and right reservoirs (electrodes) and device. The contacts (interfaces) between device and reservoirs (located at $q_{L,R}$) are necessarily subject to arbitrariness. Depending on how demanding the numerical calculations are, parts of the electrodes (as large as possible) are included in the central part and treated as accurately as possible. In the SFW method, the challenge is to determine the wave function Ψ for the total system \mathcal{S} .

Following Ref. 21, we shall consider the many-electron wave function Ψ for the total system \mathcal{S} and its associate exact energy \mathcal{E} in the presence of an applied bias

$$\mathcal{E} = \langle \Psi | H_T | \Psi \rangle = \langle \Psi | H | \Psi \rangle + \langle \Psi | W | \Psi \rangle, \quad (1)$$

where H is the Hamiltonian of the total system \mathcal{S} and W is the perturbation due to applied bias.

Within the single-particle picture, in a transport problem the (semi-infinite) reservoirs fix the electron chemical potentials $\mu_{L,R}$ at the left and right contacts, and the current flow is driven by the imbalance $\mu_L - \mu_R = eV$ created by an applied voltage. At either contact, the electron distribution is dictated by the reservoir Fermi function with the corresponding chemical potential. The attractive feature of the approach proposed in Ref. 21 is that it is based on the Wigner function, which is directly applicable to a many-body system, without the need to resort to single-particle Fermi distribution functions. For problems describable within a single-particle picture, the Wigner function method to account for open boundaries specific for transport problems has certain advantages over the conventional scattering approach.³¹⁻³³ However, these advantages are merely technical there.

For a system characterized by a many-electron wave function Ψ , the one-particle Wigner distribution function $f(q,p)$ is defined by

$$f(q,p) = \sum_{r,\sigma} \langle \Psi | a_{q-r,\sigma}^\dagger a_{q+r,\sigma} | \Psi \rangle e^{-2ipr/\hbar}. \quad (2)$$

Unlike the methods based on the NEGF, where semi-infinite leads are accounted for, the SWF method was devised to be suited for *ab initio* quantum chemical calculations, where rather than semi-infinite electrodes, only (usually very) small parts thereof can be dealt with. Instead of having an infinite extension, the wave function Ψ and the related summation over r of Eq. (2) are inherently limited in space. In this paper, we shall adopt a one-dimensional discrete representation, wherein in a lattice of size $N=2M+1$ the site index ranges from $-M$ to $+M$. In Eq. (2), $a_{l,\sigma}$ ($a_{l,\sigma}^\dagger$) denote the creation (annihilation) operators for electrons of spin σ at site l .

The open boundary conditions to be imposed should distinguish between electrons flowing into and those flowing out of the device.³¹ The distribution of the former should be determined by the reservoirs. In terms of the Wigner function, this means that, at the left (q_L) and right (q_R) boundaries between device and reservoirs $f(q_L, p_L > 0)$ and $f(q_R, p_R < 0)$ should be fixed at values dictated by the reservoirs³¹⁻³³

$$f(q_L, p_L) = f_L(p_L; \mu_L), \quad \text{for } p_L > 0, \quad (3)$$

$$f(q_R, p_R) = f_R(p_R; \mu_R), \quad \text{for } p_R < 0. \quad (4)$$

These constraints are physically plausible and have been successfully applied previously to problems treated within single-particle approximations.³¹⁻³³ The right hand sides of Eqs. (3) and (4) represent the Fermi functions of the reservoirs with the chemical potentials shifted by the bias voltage $\mu_{L,R} = \mu \pm eV/2$. Because this procedure cannot be applied for the many-body case, to determine the above $f_{L,R}$, which are basically properties of the reservoirs, it was claimed²¹ that they can be extracted from the wave function of the total system \mathcal{S} at zero bias. That is, at zero temperature, one has to determine the ground state Ψ_0 of H , then calculate f_0 by using Ψ_0 instead of Ψ in Eq. (2), and impose

$$f(q_L, p_L) = f_0(q_L, p_L), \quad \text{for } p_L > 0, \quad (5)$$

$$f(q_R, p_R) = f_0(q_R, p_R), \quad \text{for } p_R < 0. \quad (6)$$

To describe a steady state, one has to impose in addition the condition that the average J of the electric current operator³⁴ (e is the elementary charge)

$$j_l = it_l \frac{e}{\hbar} \sum_{\sigma} (a_{l+1,\sigma}^\dagger a_{l,\sigma} - a_{l,\sigma}^\dagger a_{l+1,\sigma}) \quad (7)$$

be site (l) independent

$$J_l = \langle \Psi | j_l | \Psi \rangle = J. \quad (8)$$

Above, t_l denotes the hopping integral ($-M \leq l \leq M-1$).

According to Ref. 21, the solution of the transport problem is obtained by minimizing \mathcal{E} with the supplementary constraints (5), (6), and (8) along with the normalization condition

$$\langle \Psi | \Psi \rangle = 1. \quad (9)$$

In this way, to reach its steady state, the device is allowed to optimize the Wigner distribution function of the electrons inside the device and that of the electrons flowing from it into reservoirs. (The distribution of outgoing electrons should depend only on the state of the device.)

In the present section, we shall work out the linear response approximation of the SFW method, which enables us later to compute the zero-bias conductance. That is, we shall only consider changes to the relevant quantities of the order $\mathcal{O}(V)$, caused by a small applied voltage V . The system (left reservoir, device, and right reservoir), which consists of a collection of discrete sites ranging from $-M$ to $+M$, is perturbed by a small electric perturbation

$$W = -e \sum_{l=-M}^M n_l \varphi_l, \quad (10)$$

where $n_l = \sum_{\sigma} a_{l,\sigma}^\dagger a_{l,\sigma}$ is the electron number operator and φ_l is the electric potential at site l ($\varphi_{-M} = +V/2$, $\varphi_{+M} = -V/2$). Starting with a system in the ground state Ψ_0 , we shall look for a solution Ψ describing a steady state that slightly differs from Ψ_0 . The wave function Ψ will be expanded in terms of

the complete set of eigenstates of H ($H|\Psi_n\rangle=E_n|\Psi_n\rangle$),

$$|\Psi\rangle=A_0|\Psi_0\rangle+\sum_{n\neq 0}A_n|\Psi_n\rangle, \quad (11)$$

where $A_n=\mathcal{O}(V)$ for $n\neq 0$. One should note at this point that, although the eigenstates Ψ_n can and will be chosen real, in order to satisfy the boundary conditions (5) and (6) the expansion coefficients A_n must be complex. While in general the minimization of \mathcal{E} , Eq. (1), with the constraints (5), (6), (8), and (9) represents a nonlinear problem, it considerably simplifies in the linear response limit. By introducing the Lagrange multipliers λ_{L,p_L} ($p_L>0$), λ_{R,p_R} ($p_R<0$), ω , and χ_l for the constraints (5), (6), (9), and (8), respectively, for small V the minimization amounts to solve a linear system of equations, which possesses a solution $A_0=1+\mathcal{O}(V^2)$, $A_n=\mathcal{O}(V)$ for $n\neq 0$, $\lambda_{L,p}=\mathcal{O}(V)$, $\lambda_{R,p}=\mathcal{O}(V)$, $\omega=E_0+\mathcal{O}(V)$, and $\chi_l=\mathcal{O}(V)$.

The quantities entering the minimization problem within the linear response approximations are

$$\mathcal{F}_n(q,p)\equiv\sum_{r,\sigma}\langle\Psi_n|a_{q-r,\sigma}^\dagger a_{q+r,\sigma}|\Psi_0\rangle e^{-2ipr/\hbar}, \quad (12)$$

$$\mathcal{J}_n(l)\equiv\langle\Psi_n|j_l|\Psi_0\rangle, \quad (13)$$

$$\mathcal{W}_n\equiv\langle\Psi_n|W|\Psi_0\rangle. \quad (14)$$

For the ground state ($n=0$), $\mathcal{F}_0(q,p)=f_0(q,p)$.

We shall assume (a fact justified for the models considered here) that in the absence of perturbation the Hamiltonian of the system H is invariant under inversion, and the ground state Ψ_0 is even and carries no current $\mathcal{J}_0(l)=0$. Owing to the spatial inversion of H , the eigenstates Ψ_n are either even (Ψ_g) or odd (Ψ_u). In view of the space inversion, is it natural to choose boundaries located symmetrically ($q_L=-q_R$), a mesh comprising symmetric values of positive and negative values of p ($p_L=-p_R=p>0$), and an antisymmetric applied potential profile ($\varphi_{-l}=-\varphi_l$). The quantities (12)–(14) possess the following symmetry properties:

$$\mathcal{F}_g(q_L,p)=\mathcal{F}_g(q_R,-p), \quad \mathcal{F}_u(q_L,p)=-\mathcal{F}_u(q_R,-p), \quad (15)$$

$$\mathcal{J}_g(l)=-\mathcal{J}_g(-l), \quad \mathcal{J}_u(l)=\mathcal{J}_u(-l), \quad (16)$$

$$\mathcal{W}_g=0. \quad (17)$$

Straightforward algebra shows that the equations for even (g) and odd (u) eigenstates decouple, and only odd (u) eigenstates contribute to the current

$$J=J_l=2\sum_u\text{Im}\mathcal{J}_u(l)\text{Im}A_u. \quad (18)$$

The minimization yields the following linear equations for the Lagrange multipliers $\lambda(p)\equiv[\lambda_L(p)-\lambda_R(-p)]/2$ and $\chi(j)\equiv[\chi(j)-\chi(-j)]/2$ ($j,j',p,p'>0$):

$$\begin{aligned} &\sum_{p'}\lambda(p')\sum_u\frac{1}{E_u-E_0}[\mathcal{F}_u(q_L,p')\mathcal{F}_u^*(q_L,p) \\ &\quad +\mathcal{F}_u^*(q_L,p')\mathcal{F}_u(q_L,p)] \\ &\quad +\sum_{j'=1}^{M-1}\chi(j')\sum_u\frac{1}{E_u-E_0}[\mathcal{I}_u(j')\mathcal{F}_u^*(q_L,p) \\ &\quad +\mathcal{I}_u^*(j')\mathcal{F}_u(q_L,p)]=\frac{1}{2}\sum_u\frac{\mathcal{W}_u}{E_u-E_0}[\mathcal{F}_u^*(q_L,p)+\mathcal{F}_u(q_L,p)], \end{aligned} \quad (19)$$

$$\begin{aligned} &\sum_{p'}\lambda(p')\sum_u\frac{\text{Im}\mathcal{I}_u(j)\text{Im}\mathcal{F}_u(q_L,p')}{E_u-E_0} \\ &\quad +\sum_{j'=1}^{M-1}\chi(j')\sum_u\frac{\text{Im}\mathcal{I}_u(j)\text{Im}\mathcal{I}_u(j')}{E_u-E_0}=0. \end{aligned} \quad (20)$$

Once they are determined, the relevant expansion coefficients can be computed as

$$A_u=\frac{2}{E_u-E_0}\left[-\frac{\mathcal{W}_u}{2}+\sum_p\lambda(p)\mathcal{F}_u(q_L,p)+\sum_{j=1}^{M-1}\chi(j)\mathcal{I}_u(j)\right], \quad (21)$$

which enables us to determine the electric current via Eq. (18). Notice that because \mathcal{W}_u enters linearly Eqs. (19)–(21), the current computed via Eq. (18) is proportional to the applied bias V .

A very pleasant aspect of the constrained minimization problem within linear response worked out here is the fact that Eqs. (19) and (20) represent nothing but a set of *linear* algebraic equations, which straightforwardly allows us to determine *unique* values for the Lagrange multipliers λ and χ . Therefore, the insertion into Eq. (21) yields a *unique* solution of the present minimization procedure. One should emphasize that this simplification is directly related to the linear response limit considered in the present paper. In the case of nonlinear response, the counterpart of Eqs. (19)–(21) is a series of nonlinear equations wherein the unknowns λ , χ , and A are coupled in a nontrivial way. The solution of those equations can only be obtained iteratively, and the (numerical) computation of the constraint gradient of the energy is necessary as a check for a pinned down solution.

III. MODEL

The method exposed in Sec. II is general. It will be applied to a concrete system. The physical system considered in this paper consists of a single quantum dot connected to two noninteracting leads. It can be described by the Anderson impurity model

$$\begin{aligned}
H = & \varepsilon_L \sum_{l=-1}^{-M_L} \sum_{\sigma} a_{l,\sigma}^{\dagger} a_{l,\sigma} - t_L \sum_{l=-1}^{-M_L+1} \sum_{\sigma} (a_{l,\sigma}^{\dagger} a_{l-1,\sigma} + a_{l-1,\sigma}^{\dagger} a_{l,\sigma}) \\
& + \varepsilon_R \sum_{l=1}^{M_R} \sum_{\sigma} a_{l,\sigma}^{\dagger} a_{l,\sigma} - t_R \sum_{l=1}^{M_R-1} \sum_{\sigma} (a_{l,\sigma}^{\dagger} a_{l+1,\sigma} + a_{l+1,\sigma}^{\dagger} a_{l,\sigma}) \\
& - t_{d,L} \sum_{\sigma} (a_{-1,\sigma}^{\dagger} d_{\sigma} + d_{\sigma}^{\dagger} a_{-1,\sigma}) - t_{d,R} \sum_{\sigma} (a_{+1,\sigma}^{\dagger} d_{\sigma} + d_{\sigma}^{\dagger} a_{+1,\sigma}) \\
& + \varepsilon_g \sum_{\sigma} d_{\sigma}^{\dagger} d_{\sigma} + U \hat{n}_{d,\uparrow} \hat{n}_{d,\downarrow}, \tag{22}
\end{aligned}$$

where $a_{l,\sigma}$ ($a_{l,\sigma}^{\dagger}$) denote creation (annihilation) operators for electrons of spin σ in the leads, $d_{\sigma} \equiv a_{0,\sigma}$ ($d_{\sigma}^{\dagger} \equiv a_{0,\sigma}^{\dagger}$) creates (destroys) electrons in the QD, and $\hat{n}_{d,\sigma} \equiv d_{\sigma}^{\dagger} d_{\sigma}$ are electron occupancies per spin direction. We shall consider $M_L = M_R \equiv M$, $t_L = t_R \equiv t$, $\varepsilon_L = \varepsilon_R$ (chosen as zero energy hereafter), and $t_{d,L} = t_{d,R} \equiv t_d$, and this ensures the spatial inversion assumed above. The dot energy ε_g can be tuned by varying a gate potential. In view of the particle-hole symmetry of model (22), ($\varepsilon_g = -U/2$ is the particle-hole symmetric point), we can restrict ourselves to the range $\varepsilon_g > -U/2$. The number of electrons N will be assumed equal to the number of sites ($N = 2M + 1$). The electric potential entering Eq. (10) will be assumed constant within the reservoirs $\varphi_l = -\varphi_{-l} = -V/2$ for $0 < l < M$ and zero at the dot location $\varphi_0 = 0$.

In isolated electrodes ($t_d = 0$), the single-particle energies lie symmetrically around $\varepsilon = 0$. Therefore, in order to eliminate energy corrections $\sim t/M$ in small clusters, it is advantageous to consider reservoirs with an odd number of sites M .^{35,36} In the noninteracting case ($U = 0$), the resonant tunneling at the Fermi energy ($\mu = 0$) is favored for odd M . In the presence of interaction, the Kondo effect occurs when the dot spin couples with electrons of the leads at the Fermi level. This coupling is favored if the leads possess single electron levels of zero energy, and this is the case for reservoirs consisting of an odd number (M) of sites.

Although the numerical values used for the results presented in this or in the next Sec. IV do not represent a special choice, we prefer to employ values corresponding to a possible physical realization of the above model, namely, chains of QDs of silver. Such QDs were experimentally fabricated.^{37–44} Their properties can be tuned in wide ranges by varying the dot diameter ($2R$) and interdot spacing (D),^{37–44} and the parameters are well documented in a series of experimental and theoretical works.^{37,41,45,46} For interdot spacings up to say, $D/2R \lesssim 1.3$, electron correlations are not important.^{46–48} Therefore, the reservoirs can be modeled, e.g., by chains of nearly touching QDs ($D/2R \approx 1.07$, $t = 1$ eV).

In principle, the boundaries could be chosen at $0 < q_R = -q_L < M$. Unless otherwise specified, we shall choose $q_{L,R} = \mp 2$. It amounts to consider the central part to consist of the QD and two additional sites, one at either side of the “device,” represented by the QD of interest. This bears the most resemblance to usual quantum chemical approaches to molecular transport, wherein the smallest possible parts of electrodes are included in the central part. In Eq. (2), there are $n_{q_L} = 2(M + q_L) + 1$ values of r such that the values of site

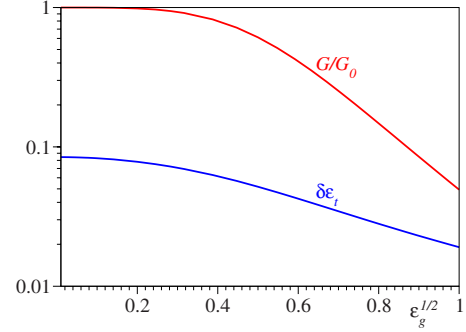


FIG. 1. (Color online) Results for the normalized conductance G/G_0 and lowest excitation energy $\delta\varepsilon_t$ (tunneling splitting) obtained by exact diagonalization in the uncorrelated system ($U = 0$) for chains with 63 sites, $t = 1$, and $t_d = 0.4$. Note the logarithmic scale on the ordinate and the square root of the dot energy (=energy barrier) ε_g on the abscissa. The linearity of the two curves at larger ε_g confirms the interpretation within the tunneling model.

indices are $q_L \pm r = 0, \pm 1, \dots, \pm(M + q_L)$. According to the careful analysis of Ref. 31, the values of p in Eq. (2) should span the first Brillouin zone of the reciprocal space of $2r$.

IV. CONDUCTANCE THROUGH A POINT CONTACT IN THE ABSENCE OF CORRELATIONS

Let us start with the noninteracting case, amounting to switch off the Coulomb interaction ($U = 0$) in Eq. (22). This represents the textbook case of conduction through a single level system.¹¹ By approaching the resonance $\varepsilon_g \rightarrow 0$, the transmission becomes perfect. The curve of the conductance $G(\varepsilon_g)$ exhibits a peak characterized by a height $G(0) = G_0$ and a half-width parameter $\Gamma = 2t_d^2/t$.

For the numerical calculations in this section, we shall choose a value $t_d/t = 0.4$. This corresponds to an Ag-QD chain, with a QD in the middle slightly more distant ($D'/2R = 1.24$) from its two neighbors than the other QDs in the chains ($D/2R = 1.07$, cf. Sec. III).

In the case of identical reservoirs and contacts, the zero-bias conductance can be obtained from the Friedel-Langreth sum rule^{49–52}

$$G/G_0 = \sin^2(\pi n_d/2), \tag{23}$$

where $G_0 \equiv 2e^2/h$ is the conductance quantum. The dot occupancy per spin direction $n_d = \sum_{\sigma} \langle \Psi_0 | \hat{n}_{d,\sigma} | \Psi_0 \rangle$ will be computed by numerical exact diagonalization.

In Fig. 1, we present numerical results obtained for 63 sites by means of Eq. (23), which show a peak in the conductance $G(\varepsilon_g)$ with a half width at half maximum in very good agreement with the formula $\Gamma = 2t_d^2/t$. These results are in accord with the fact that the single-particle quantum tunneling constitutes the underlying physical phenomenon: At sufficiently large values of ε_g , the curve for $\log G(\varepsilon_g)$ in Fig. 1 varies linearly with $\varepsilon_g^{1/2}$, as expected for the transmission coefficient through an energy barrier ε_g . The lowest excitation energy, also shown in Fig. 1, displays a similar dependence, which confirms that it plays the role of a tunneling splitting energy.

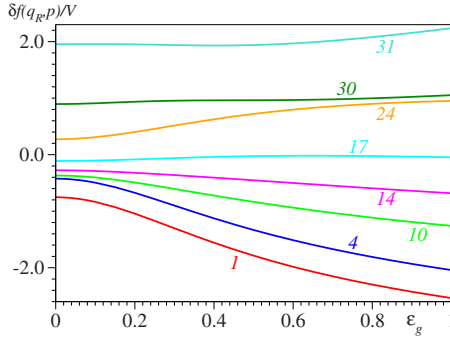


FIG. 2. (Color online) The difference $\delta f(q_R, p) \equiv f(q_R, p) - f_0(q_R, p)$ (in arbitrary units) plotted versus gate potential ϵ_g for 63 sites, $t=1$, $t_I=0.4$. The nonvanishing values at the right interface q_R and positive momenta p indicate that the Wigner distribution function of outgoing electrons is free. The values of k ($p=k\pi/n_{q_L}$) are given in the legend.

The curve of conductance for chains with 63 sites depicted in Fig. 1 is very close to the exact result for infinite chains presented in Fig. 5 of Ref. 36. It has been shown there that the latter result agrees very well with the time-dependent DMRG result for 64 sites.³⁶ The size $N=63$ chosen by us is the closest to chain size $N=64$ used in the time-dependent DMRG calculations compatible with our choice ($N=2M+1$, with odd M , cf. Sec. III).

We shall now present the results of the SWF method discussed in Sec. II. From the point of view of the computation time, large chain sizes are more prohibitive for the SWF method than for exact diagonalization. Indeed, by inspecting Eqs. (18)–(21) one can see that the computing time for J scales as N^6 in the noninteracting case, where the number of relevant excitations scales as N^2 . Because the Hamiltonian (22) is quadratic in the noninteracting case, exact numerical diagonalization can be straightforwardly carried out even for very long chains, e.g., much longer than those that can be handled by the time-dependent DMRG.

Figure 2 represents a counterpart of the bottom panel of Fig. 1 of Ref. 21 and illustrates a characteristic feature of the SWF method discussed in Sec. II: the reservoirs only constrain the Wigner distribution function of incoming electrons while the distribution of outgoing electrons is free. For instance, at the right interface $\delta f(q_R, p) \equiv f(q_R, p) - f_0(q_R, p)$ is zero for $p < 0$ [in accord with Eq. (6)] but has nonvanishing values for $p > 0$. Curves for the latter case are shown in Fig. 2, depicted for several positive values of p .

We shall now compare the exact results with those of the SWF method. In Fig. 3, the SWF curve for zero-bias conductance is plotted along with the exact curve. As one can clearly see there, the SWF curve looks completely different, bearing no resemblance with the exact curve. Most unphysically, the SWF conductance vanishes for resonant tunneling ($\epsilon_g=0$), where it should attain the maximum value $G=G_0$.

To compute the SWF curve of Fig. 3, we have chosen $q_L=-2$ and $q_R=2$. A nontrivial realistic *ab initio* calculation is so demanding that, besides the device (a molecule or a few QDs), if at all, only small parts of the electrodes can be accounted for in the heaviest part of the computation. Therefore, practically no or very limited freedom remains to

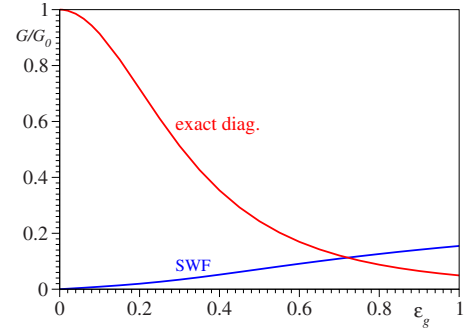


FIG. 3. (Color online) Results on the normalized conductance G/G_0 obtained by exact diagonalization and the method based on the Wigner function for 63 sites in the absence of correlations $U=0$ (same parameters as in Fig. 1).

choose the boundaries $q_{L,R}$. The fact that in the present case the eigenvalue problem can be solved exactly for large systems \mathcal{S} enables us to flexibly change $q_{L,R}$ and to inspect the impact on the solution, and, maybe to make it have some resemblance to the exact one. In Fig. 4, we present results derived by choosing different $q_{L,R}$. For all choices, the optimization yields minimum values of the total energy \mathcal{E} , Eq. (1), below the value \mathcal{E}_0 corresponding to the trivial situation $A_n=0$, $\forall n \neq 0$, i.e., the “condensation” energy $\delta\mathcal{W} \equiv \mathcal{E} - \mathcal{E}_0$ is negative. However, the conductance changes only by factors of the order of unity. Definitely, it cannot be made more akin to the exact G .

The curves presented in the above Figs. 2–4 have been deduced by constraining the solution to satisfy the equation of continuity, as discussed in Sec. II. In Fig. 5, results obtained by imposing the equation of continuity (depicted by the line denoted by *uniform*) are compared with those derived without imposing this equation. As is visible there, the values of the electric current do display a significant dependence on site. The latter is indicated by the numbers in the legend of Fig. 5. Neither the value of the current through the QD nor the average along the chain (label 0 and *average*, respectively) coincides or reasonably approximates that deduced by imposing the equation of continuity. It was claimed

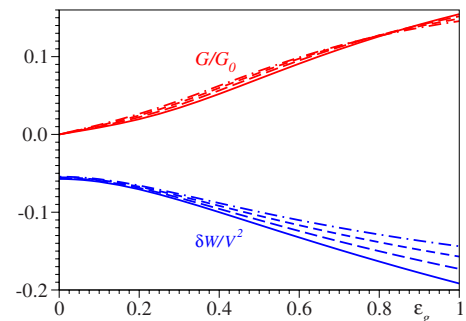


FIG. 4. (Color online) Results for the conductance G/G_0 and the bias-induced condensation energy $\delta\mathcal{W}$ (the latter in arbitrary units) obtained by means of the SWF method for boundaries chosen at $q_R=-q_L=2, 3, 4$, and 5 (values increasing upwards for the G curves and downwards for the $\delta\mathcal{W}$ curves at, say, $\epsilon_g=0.5$). Noteworthy, the conductance does not sensitively depend on the choice of boundaries.

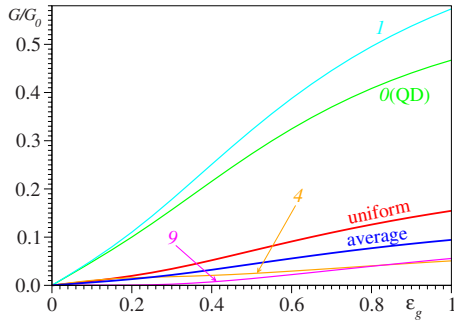


FIG. 5. (Color online) SWF results for the conductance G/G_0 of the chain with 63 sites at $t=1$ and $t_d=0.4$. The curves computed without imposing the continuity equation exhibit a strong site-dependent current and substantially depart from that labeled by *uniform*, computed by imposing this equation. Nor the average taken along the chain (label *average*) represents a satisfactory approximation of the latter. The number of site q in the chain is specified in the legend. The dot is located at $q=0$.

that, although in principle necessary because of certain approximations (see Sec. VI for more details), there was no need to impose the equation of continuity for the calculations reported in Refs. 21 and 22. Obviously, the fact that in our case the minimization without imposing Eq. (8) leads to a solution for Ψ that violates the equation of continuity is not the result of any approximation: except for the SWF method itself, our results are affected by no further approximation. To conclude, Fig. 5 demonstrates that the SWF method does not automatically satisfy the continuity equation, not even approximately.

V. CONDUCTANCE THROUGH A POINT CONTACT IN THE PRESENCE OF CORRELATIONS

In this section we shall apply the SWF method exposed in Sec. II for the case of nonvanishing U , where correlations are known to play an important role. The physics of model (22) with $U \neq 0$ is also well understood.⁵³ For strong interaction (U) and low temperatures, by varying the gate potential ε_g , one observes plateaus of well defined dot charge, corresponding to a dot that is empty, singly, and doubly occupied: $n_d=0$ ($0 < \varepsilon_d$), $n_d=1$ ($-U < \varepsilon_d < 0$), and $n_d=2$ ($\varepsilon_d < -U$), respectively. This behavior can be demonstrated by exact numerical diagonalization in small clusters, as illustrated by the curves of Fig. 6.

For low temperatures but above the so-called Kondo temperature T_K (often much smaller than 1 K), the conductance $G(\varepsilon_g)$ exhibits two narrow Coulomb blockade peaks located at $\varepsilon_g = -U$ and $\varepsilon_g = 0$, while in between it almost vanishes (Coulomb valley). By decreasing the temperature below T_K , correlation effects in the singly occupied state yield a sharp (Kondo) resonance in the density of states at the Fermi level, and this gives rise to a characteristic plateau of width $\sim U$ in the curve of G versus ε_g . In the middle of the Coulomb valley ($\varepsilon_g = -U/2$), perfect transmission occurs, leading to the ideal conductance value $G_0 = 2e^2/h$ (unitary limit).

Numerous results obtained for the model (22) by considering semi-infinite leads were published in the literature, see,

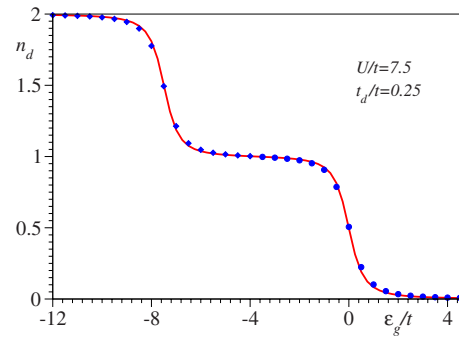


FIG. 6. (Color online) Dot occupancy n_d computed by exact diagonalization for 7- and 11-site clusters (solid lines and points, respectively) plotted versus dot energy ε_g . Notice the small difference between the results for 7 and 11 sites, indicating that finite-size effects play a reduced role.

e.g., Refs. 36, 54, and 55. A comparison between the results for semi-infinite leads and the SWF method would make no sense. At zero temperature, the case for which the SWF method was developed, in the range $-U \lesssim \varepsilon_g \lesssim 0$ for the realistic case of semi-infinite electrodes the conductance is dominated by the Kondo plateau. Its formation requires chain sizes larger than the Kondo cloud, which extends over a number of sites $\xi_K \sim t/T_K$. The latter rapidly grows (exponentially for large U) beyond the sizes, which neither the exact diagonalization, nor the SWF, or often even the DMRG approach,³⁶ can handle. No Kondo peak can be formed for chains shorter than the Kondo screening length ξ_K . However, in short chains the $G(\varepsilon_g)$ curve should still display the Coulomb blockade peaks at $\varepsilon_g = 0$ and $\varepsilon_g = -U$.

Although the clusters considered in this section comprise a small number of sites, the results are significant. Since our main purpose here is to address the issue of the validity of the SWF method, we do not intend to discuss finite-size effects here. However, we do not expect that they are essential: the inspection of Fig. 6 reveals that the differences between chains with seven ($M=3$) and eleven ($M=5$) sites are not substantial.

The primary reason why we restrict ourselves to chains with seven sites is technical, but this also rises supplementary doubts on the applicability of the SWF methods for systems of interest for molecular electronics. Equation (11) is an expansion over the complete set of eigenstates of H and, according to Eq. (18), in principle all eigenstates of odd parity contribute to the current. Calculations contradict the naive expectation that in the linear response approximation only a reduced number of excited states are important. For the couplings U employed in Fig. 7, out of a total of 1225 states with spin projection $S_z = +1/2$, the first 300 states are not always enough to reach convergence. For eleven-site chains (the next larger size of interest), there are 213 444 eigenstates with $S_z = +1/2$. One would probably need to target many thousands thereof in order to get the matrix elements necessary for convergent results. For this formidable task, one should run the Lanczos procedure three times, and this separately for each of the matrix elements entering Eqs. (12)–(14), in a manner similar to but more involved than that employed to compute frequencies and intensities of optical

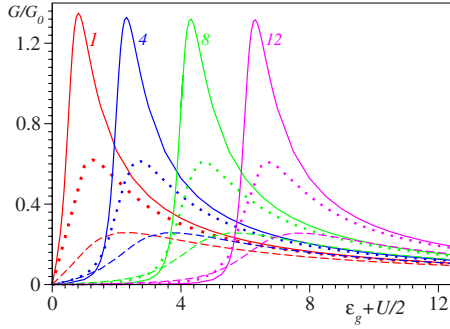


FIG. 7. (Color online) Coulomb blockade peaks of the zero-bias conductance for seven-site clusters as predicted by the SWF method. The solid, dotted, and dashed lines correspond to the values $t_d=0.125, 0.25,$ and 0.5 respectively. The values of U are given in the legend and $t=1$. Notice that, unphysically, the maximum conductance is predicted to increase with decreasing t_d even beyond the ideal value G_0 ($G/G_0 > 1$).

lines.^{47,48,56,57} The method of only computing convoluted spectra by means of the continued fraction algorithm^{58–60} is inadequate for this purpose.

Our results on the conductance computed by means of the SWF method are collected in Fig. 7. (Notice that only the halves of the curves situated at the right of the particle-hole symmetric point $\varepsilon_g + U/2 = 0$ are shown.) As one can see there, the curves for the conductance, calculated for several values of U and t_d , exhibit maxima at the gate potential values $\varepsilon_g \geq 0$ ($\varepsilon_g + U/2 \geq U/2$), i.e., at the position where the Coulomb blockade peaks are expected. Their distance from the ideal Coulomb blockade location increases with t_d ; a behavior similar to that of their width. While this behavior is physically plausible, unfortunately, the prediction of the SWF method for the height of the peaks is quite unphysical: the height is found to vary roughly inversely proportional to t_d . The consequence of this dependence is that, as visible in Fig. 7, the height of the G peak even attains values exceeding the ideal value G_0 . To conclude this section, the results of the SWF method are unphysical; the conductance of correlated systems evaluated by this method cannot be trusted.

VI. DISCUSSION

A minimal requirement for any many-body approach of electric transport at nanoscale is to reproduce the Landauer theory in the absence of correlations and to correctly describe the zero-bias conductance of the linear response theory. Although these represent two well established limits (see, for example, Ref. 20), the authors of Refs. 21, 29, and 30 did not show that their (SWF) method is compatible to them. In the preceding Secs. IV and V we have unambiguously demonstrated that the SWF method is *incompatible* to the two aforementioned limits.

We still have two comments on the SFW method. They concern this method in general and are not related to the linear response limit. First, in Ref. 22, it was claimed that the imposition of Eq. (8) is necessary because the continuity equation $\partial\rho/\partial t + \nabla \cdot \mathbf{j} = 0$, derived from the Schrödinger equation in the presence of local interactions, does not hold for

nonlocal interactions. Accordingly, position-dependent currents could be an effect of *ab initio* molecular electronics calculations employing nonlocal effective core potentials or pseudopotentials, or a result of truncating the molecular orbital basis set or the CI. While all these may in general be sources of violating the continuity equation, for the SWF method there still exists another reason to impose the constraints (8) in a steady state. The wave function Ψ determined by means of the SWF method does not represent an eigenstate of the Hamiltonian. Ψ is time independent only because the formalism is time independent, and not the result e.g., of taking the limit $t \rightarrow \infty$ to get a steady state. No demonstration has been given in the works dealing with the SWF method^{21,22,29,30,61} that the minimization procedure without imposing Eq. (8) yields a solution compatible with the continuity equation. While the imposition of Eq. (8) is seemingly unnecessary for the case considered in Ref. 22, there is no rationale for this in general. For illustration, we have presented a counter example in Sec. IV. The equation of continuity $\partial n_l / \partial t = (i/\hbar)[n_l, H] = -j_l + j_{l-1}$ (cf. Ref. 34) holds for the model Hamiltonian (22), and nevertheless the current computed without imposing Eq. (8) is strongly site dependent.

The second and more important point concerns the manner of imposing boundary conditions in Ref. 21. In the approaches based on the Wigner function within the single-particle approximation the influence of the applied electric field is accounted for both at the boundary conditions, via the shift $\mu_L - \mu_R = eV$ [cf. Eqs. (3) and (4)] and on the electron dynamics within the device.^{31–33} Within the methods based on the NEGF the applied voltage is usually considered solely via the chemical potential imbalance, and many-body¹⁰ methods are employed to treat correlation effects due to interactions within the device without applied field. In both cases, the applied bias represents the driving force of current flow. In the SWF method, the effect of the applied field at the boundaries is entirely neglected [cf. Eqs. (5) and (6)]. Let us suppose that (i) we would be able to reliably solve the minimization problem as prescribed by the SWF method and exactly (or at least very accurately) determine Ψ for very large systems, including large parts of the reservoirs (assumed identical), and (ii) in the latter the single-particle description applies. Then, according to Eqs. (5) and (6), the Wigner functions at the boundaries would reduce to the Fermi distribution functions of the left and right reservoirs characterized by the *same* chemical potential μ . This would imply that there would be no difference between incoming electrons from the left and right reservoirs. Then, it is not at all surprising, e.g., that in the extreme case, where all sites are noninteracting and identical ($U=0$ and $t_d=t$), instead of being maximum, $G=G_0$, the conductance vanishes for $\varepsilon_g=0$, as visible for the SWF curves of Figs. 3–5. In reality, the correct wave function Ψ describing the steady-state current flow should yield a Wigner function that reduces at the boundaries to the Fermi distribution functions characterized by different chemical potentials $\mu_{L,R} = \mu \pm eV/2$.

The vanishing zero-bias conductance for $\varepsilon_g=0$ (Fig. 3) is perhaps the most striking and unphysical result of the SWF method. It might be tempting to ascribe the vanishing (zero-bias) conductance to the fact that the SWF method uses finite

electrodes rather than (practically) infinite electrodes and does not include self energies or other level broadenings. Since our primary aim in this paper is to check the validity of the SWF method, we have faithfully translated this approach as proposed in Ref. 21 to concrete cases. However, we do not believe that the above fact is the source of quite unphysical predictions. The time-dependent DMRG method¹²⁻¹⁴ is in this respect similar to the SWF method, since it also considers finite electrodes, but is able to correctly reproduce exact results, as discussed in Sec. IV. Because the aforementioned vanishing zero-bias conductance is quite unphysical, we think that it would make little sense to ask whether the current at low voltages is proportional to a higher power of V within the SWF approach: this would be yet another unphysical prediction. However, in view of the considerations of the preceding paragraph on the imposition of the boundary conditions, we believe that even higher order conductivities are suppressed.

Since the above analysis reveals that the boundary conditions (5) and (6) are inadequate, attempting to mend the SWF method would be desirable. In view of the above considerations, perhaps the most natural attempt would be to modify Eqs. (5) and (6) by using instead of Ψ_0 the ground state Φ_0 of the system in the presence of the applied potential, i.e., $H_T|\Phi_0\rangle = E_{T,0}|\Phi_0\rangle$. Although the Wigner functions entering the right hand side of Eqs. (5) and (6), calculated by using Φ_0 instead of Ψ_0 , do not necessarily reduce to the left and right Fermi distributions, this procedure would at least account for the chemical potential imbalance at the boundaries. However, as revealed by a straightforward analysis, this modification does not yield the desired improvement: the solution of the minimization is just $\Psi = \Phi_0$. This solution obviously satisfies the boundary constraints (5) and (6) as well as the continuity equation (electrical perturbations only depend on electron density), and, being the ground state of H_T , it trivially minimizes \mathcal{E} of Eq. (1). This result is obviously general, i.e., it holds beyond the linear response approximation. Still, as a verification, we have performed the modification $\Psi_0 \rightarrow \Phi_0$ in the right hand side of Eqs. (5) and (6) and carried out straightforward calculations within the linear response approximation. They yield $|\Psi\rangle = |\Psi_0\rangle + \sum_{n \neq 0} \mathcal{W}_n / (E_0 - E_n) |\Psi_n\rangle$, and in the right hand side one immediately recognizes the ground state Φ_0 of $H_T = H + W$ in the first order of perturbation theory. Unless the system is superconducting, the current (conductance) vanishes in the state described by the wave function $\Psi = \Phi_0$. So, even with this ‘‘remedy,’’ the SWF method is unable to describe electric transport through nanosystems.

VII. CONCLUSION

Several recent studies proposed and applied a many-body time-independent method to compute steady-state electric transport in molecular systems, whose key ingredient was the

formulation of the boundary conditions in terms of the Wigner distribution function.^{21,22,29,30,61} The fact that this approach yielded values of the electric current through molecules comparable with those measured in experiments, which are usually orders of magnitudes lower than the predictions of other theoretical treatments, was considered very encouraging. However, the mere fact that a theoretical method compares favorably with experiments cannot be taken as support for its correctness. It should also be able to correctly reproduce well established results.

In this paper, we have presented results demonstrating that the SWF method is unable to reliably evaluate the zero-bias conductance of the simplest uncorrelated and correlated systems of interest for molecular and nanoscopic systems, namely, a single QD. It fails to retrieve the result $G = G_0$ for resonant tunneling through a single QD without correlations, where it predicts a vanishing conductance instead. In the presence of correlations, the conductance at the peaks of Coulomb blockade is unphysically predicted to increase with decreasing dot-electrode coupling (t_d) and can even exceed the conductance quantum G_0 .

While the idea of formulating boundary conditions in terms of the Wigner function for correlated many-body systems is interesting, the manner in which it was imposed in Ref. 21 turns out to be inappropriate. It misses the fact that, in accord with our physical understanding, the current flow is due to an *asymmetric* injection of electrons from reservoirs into the device, and that injected electrons are very well described by Fermi distributions with different chemical potentials. Moreover, as results from the analysis at the end of Sec. VI, unfortunately there is no simple remedy of the SWF method; the modification of the boundary conditions *in the spirit* of Ref. 21 such as to account for a nonvanishing chemical potential shift does not yield the desired improvement.

In addition, as a side note, we believe that the very fact that astonishingly numerous states with high excitation energies are found to contribute to the conductance in the *linear approximation* is an indication that the SWF method, even if it were physically sound, would be of little pragmatical use for strongly correlated nanosystems, because it would be hardly conceivable that *ab initio* calculations for real molecular systems, by far more complex than the presently considered model, could provide a wave function Ψ with the accuracy needed for reaching reliable convergent results. These considerations raise doubts on the possibility to develop a viable SWF approach for the electric transport through nanoscopic and molecular systems.

ACKNOWLEDGMENT

The authors acknowledge with thanks the financial support for this work provided by the Deutsche Forschungsgemeinschaft (DFG).

- *Also at National Institute for Lasers, Plasma, and Radiation Physics, ISS, POB MG-23, RO 077125 Bucharest, Romania: ioan.baldea@pci.uni-heidelberg.de
- ¹J. Heurich, J. C. Cuevas, W. Wenzel, and G. Schön, *Phys. Rev. Lett.* **88**, 256803 (2002).
 - ²A. Nitzan and M. A. Ratner, *Science* **300**, 1384 (2003).
 - ³K. Stokbro, J. Taylor, M. Brandbyge, J.-L. Mozos, and P. Ordejón, *Comput. Mater. Sci.* **27**, 151 (2003).
 - ⁴M. A. Reed, C. Zhou, C. J. Muller, T. P. Burgin, and J. M. Tour, *Science* **278**, 252 (1997).
 - ⁵X. Xiao, B. Xu, and N. Tao, *Nano Lett.* **4**, 267 (2004).
 - ⁶T. Dadosh, Y. Gordin, R. Krahne, I. Khivrich, D. Mahalu, V. Frydman, J. Sperling, A. Yacoby, and I. Bar-Joseph, *Nature (London)* **436**, 677 (2005).
 - ⁷M. Tsutsui, Y. Teramae, S. Kurokawa, and A. Sakai, *Appl. Phys. Lett.* **89**, 163111 (2006).
 - ⁸R. Landauer, *Philos. Mag.* **21**, 863 (1970).
 - ⁹M. Büttiker, Y. Imry, R. Landauer, and S. Pinhas, *Phys. Rev. B* **31**, 6207 (1985).
 - ¹⁰H. Haug and A.-P. Jauho, *Quantum Kinetics in Transport and Optics of Semiconductors*, Springer Series in Solid-State Sciences Vol. 123 (Springer, Berlin, Heidelberg, New York, 1996).
 - ¹¹S. Datta, *Quantum Transport: Atom to Transistor* (Cambridge University Press, Cambridge, England, 2005).
 - ¹²S. R. White and A. E. Feiguin, *Phys. Rev. Lett.* **93**, 076401 (2004).
 - ¹³A. J. Daley, C. Kollath, U. Schollwöck, and G. Vidal, *J. Stat. Mech.: Theory Exp.* (2004) P04005.
 - ¹⁴A. E. Feiguin and S. R. White, *Phys. Rev. B* **72**, 020404(R) (2005).
 - ¹⁵R. Bulla, T. A. Costi, and T. Pruschke, *Rev. Mod. Phys.* **80**, 395 (2008).
 - ¹⁶J. Taylor, H. Guo, and J. Wang, *Phys. Rev. B* **63**, 245407 (2001).
 - ¹⁷M. Brandbyge, J.-L. Mozos, P. Ordejón, J. Taylor, and K. Stokbro, *Phys. Rev. B* **65**, 165401 (2002).
 - ¹⁸A. R. Rocha, V. M. Garcia-Suarez, S. Bailey, C. Lambert, J. Ferrer, and S. Sanvito, *Phys. Rev. B* **73**, 085414 (2006).
 - ¹⁹M. H. Hettler, W. Wenzel, M. R. Wegewijs, and H. Schoeller, *Phys. Rev. Lett.* **90**, 076805 (2003).
 - ²⁰R. Baer and D. Neuhauser, *Chem. Phys. Lett.* **374**, 459 (2003).
 - ²¹P. Delaney and J. C. Greer, *Phys. Rev. Lett.* **93**, 036805 (2004).
 - ²²P. Delaney and J. C. Greer, *Int. J. Quantum Chem.* **100**, 1163 (2004).
 - ²³B. Muralidharan, A. W. Ghosh, and S. Datta, *Phys. Rev. B* **73**, 155410 (2006).
 - ²⁴K. S. Thygesen and A. Rubio, *J. Chem. Phys.* **126**, 091101 (2007).
 - ²⁵G. Vignale and M. Rasolt, *Phys. Rev. Lett.* **59**, 2360 (1987).
 - ²⁶G. Vignale and M. Rasolt, *Phys. Rev. B* **37**, 10685 (1988).
 - ²⁷C. Toher and S. Sanvito, *Phys. Rev. Lett.* **99**, 056801 (2007).
 - ²⁸S.-H. Ke, H. U. Baranger, and W. Yang, *J. Chem. Phys.* **126**, 201102 (2007).
 - ²⁹G. Fagas and J. C. Greer, *Nanotechnology* **18**, 424010 (2007).
 - ³⁰G. Fagas, P. Delaney, and J. C. Greer, *Phys. Rev. B* **73**, 241314(R) (2006).
 - ³¹W. R. Frensley, *Rev. Mod. Phys.* **63**, 215 (1991).
 - ³²W. R. Frensley, *Phys. Rev. Lett.* **57**, 2853 (1986).
 - ³³W. R. Frensley, *Phys. Rev. Lett.* **60**, 1589 (1988).
 - ³⁴C. Caroli, R. Combescot, P. Nozières, and D. Saint-James, *J. Phys. C* **4**, 916 (1971).
 - ³⁵G. Chiappe and J. A. Vergés, *J. Phys.: Condens. Matter* **15**, 8805 (2003).
 - ³⁶K. A. Al-Hassanieh, A. E. Feiguin, J. A. Riera, C. A. Busser, and E. Dagotto, *Phys. Rev. B* **73**, 195304 (2006).
 - ³⁷C. P. Collier, R. J. Saykally, J. J. Shiang, S. E. Henrichs, and J. R. Heath, *Science* **277**, 1978 (1997).
 - ³⁸J. Heath, C. Knobler, and D. Leff, *J. Phys. Chem. B* **101**, 189 (1997).
 - ³⁹G. Markovich, C. P. Collier, and J. R. Heath, *Phys. Rev. Lett.* **80**, 3807 (1998).
 - ⁴⁰J. Shiang, J. Heath, C. Collier, and R. Saykally, *J. Phys. Chem. B* **102**, 3425 (1998).
 - ⁴¹G. Medeiros-Ribeiro, D. A. A. Ohlberg, R. S. Williams, and J. R. Heath, *Phys. Rev. B* **59**, 1633 (1999).
 - ⁴²S. Henrichs, C. Collier, R. Saykally, Y. Shen, and J. Heath, *J. Am. Chem. Soc.* **122**, 4077 (2000).
 - ⁴³J. Sampaio, K. Beverly, and J. Heath, *J. Phys. Chem. B* **105**, 8797 (2001).
 - ⁴⁴K. Beverly, J. Sampaio, and J. Heath, *J. Phys. Chem. B* **106**, 2131 (2002).
 - ⁴⁵F. Remacle, C. P. Collier, J. R. Heath, and R. D. Levine, *Chem. Phys. Lett.* **291**, 453 (1998).
 - ⁴⁶I. Bâldea and L. S. Cederbaum, *Phys. Rev. Lett.* **89**, 133003 (2002).
 - ⁴⁷I. Bâldea and L. S. Cederbaum, *Phys. Rev. B* **75**, 125323 (2007).
 - ⁴⁸I. Bâldea and L. S. Cederbaum, *Phys. Rev. B* **77**, 165339 (2008).
 - ⁴⁹D. C. Langreth, *Phys. Rev.* **150**, 516 (1966).
 - ⁵⁰H. Shiba, *Prog. Theor. Phys.* **54**, 967 (1975).
 - ⁵¹Y. Meir and N. S. Wingreen, *Phys. Rev. Lett.* **68**, 2512 (1992).
 - ⁵²A.-P. Jauho, N. S. Wingreen, and Y. Meir, *Phys. Rev. B* **50**, 5528 (1994).
 - ⁵³T. K. Ng and P. A. Lee, *Phys. Rev. Lett.* **61**, 1768 (1988).
 - ⁵⁴W. Izumida, O. Sakai, and S. Suzuki, *J. Phys. Soc. Jpn.* **70**, 1045 (2001).
 - ⁵⁵T. A. Costi, *Phys. Rev. B* **64**, 241310(R) (2001).
 - ⁵⁶H. Köppel, W. Domcke, and L. S. Cederbaum, *Adv. Chem. Phys.* **57**, 59 (1984).
 - ⁵⁷I. Bâldea, H. Köppel, and L. S. Cederbaum, *Phys. Rev. B* **55**, 1481 (1997).
 - ⁵⁸D. Bullet, R. Haydock, V. Heine, and M. J. Kelly, in *Solid State Physics*, edited by H. Erhenreich, F. Seitz, and D. Turnbull (Academic, New York, 1980).
 - ⁵⁹P. Fulde, *Electron Correlations in Molecules and Solids*, Springer Series in Solid-State Sciences Vol. 100 (Springer-Verlag, Berlin, 1991).
 - ⁶⁰E. Dagotto, *Rev. Mod. Phys.* **66**, 763 (1994).
 - ⁶¹P. Delaney and J. C. Greer, *Proc. R. Soc. London, Ser. A* **462**, 117 (2006).